Article

Geophysical investigation of Ankashasha dam site, Southern Ethiopia

Gebre Gidey Weldeabzgi[1], **Mulugeta Markos Tediso**[2]
[1]Depatment of Natural Resource Management, Dambi Dollo University, Ethiopia
[2]Department of Physics, Dambi Dollo University, Ethiopia
E-mail: gebregidey09@gmail.com

Received 7 February 2023; *Accepted 1 March 2023*; *Published online 10 March 2023*; *Published 1 June 2023*

Abstract
The study area, Ankashasha dam site is found in South Nations, Nationalities and Peoples Regional state of Ethiopia. The overall objective of geophysical investigations in the study area is to assist geological studies to determine the depth of bedrock and estimate the probable seepage that might encounter dam reservoir areas. Vertical Electrical Sounding (VES) and two-dimensional electrical resistivity imaging survey methods were used to assess the safety of the Ankashasha dam. The data were acquired from four VES points using Schlumberger cathode arrays with supreme half current electrode spacing, and two-dimensional electrical resistivity imaging three profile data points were analyzed qualitatively and quantitatively to understand the geology and identify aquifer bearing horizons. The qualitative analysis of VES data was accomplished by using curves, apparent resistivity, pseudo-depths, and the quantitative interpretations of the VES data were constructed by the VES data using IpI-res3, IPI2win and Surfer software and constructing geo-electric section sideways profiles using the result from VES point interpretations and lithological information from the Bedesa borehole. The VES results of the data revealed three geoelectric layers that differ in degree of fracturing, weathering and formation. The bedrock is closer to the surface on the delineated fracture boundaries on the geo-electric section of the NE flanks of the axis. The overburden materials consist of seepage flow paths that widen northeastwards parallel to clay, sandy clay and clayey sand. Seismic refraction work should be forwarded since the area is seismically active to map the structures and determine parameters such as densities of each layer, weak zones, depth to contacts and others.

Keywords electrical resistivity; lithology; geophysical; topography; resistivity imaging.

Computational Ecology and Software
ISSN 2220-721X
URL: http://www.iaees.org/publications/journals/ces/online-version.asp
RSS: http://www.iaees.org/publications/journals/ces/rss.xml
E-mail: ces@iaees.org
Editor-in-Chief: WenJun Zhang
Publisher: International Academy of Ecology and Environmental Sciences

1 Introduction

A barrage can be assumed as a configuration built transversely a stream or watercourse pointed at blockading and inspirational the aquatic equal to generate a basin of water (Moisio et al., 2021). This basin can be used for numerous determinations: downpour controller, irrigation, power age band, triangulation, pour regularisation,

city and manufacturing source, fish husbandry, restoration, the vacation industry, manufacturing stakeouts, among others goalmouths. Inappropriately, complications with barriers are recurrent. Scientific enlargement has provided enhancements over the period, but there is motionless intelligence of glitches accompanying barrages (Fisseha et al., 2021). Geophysics is an imperative instrument for the examination of arrangements such as barrages. Numerous circumstance studies of barrages reviewed by geophysical approaches have been testified, but the electric resistivity technique is slightly browbeaten for examinations of dams (Zhang et al., 2021). Inspected reasons for international dam disappointments revealed that 25% of the catastrophes were geotechnical difficulties related to leakage, insufficient seepage cutoff, responsibilities, reimbursements, and victories. The current study solicits the electric resistivity technique for research within the physique of a trivial ground dam, with the determination of classifying lithology, structures, bedrock and the nature of its water percolation areas.

A dam site is positioned in the Chiro stream gorge composed of soft to medium-strong welded tuff, and its surface is covered by sand (Fig. 1). Generally, the upstream, downstream and reservoir embankment areas are overlain by rock units of recent rift valley pyroclastic formations, such as tuff, volcanic sand and pumice deposits. This, in turn, is underlain by the formation of rock units of fractured ignimbrite beds. In addition, the depth of Ignimbrite beneath the gorge is not known. The outcrops of the formation and the counterpart are observed along the stream bank.

Fig. 1 The photo was taken at Chiro stream NE of the valley side view.

2 Materials and Methods

2.1 Location and accessibility

The dam site is found in the AnkaShahsara kebele which is located at 12 km west of Bedesa at the side off-road from the main Sodo Moricho highway road in the Wolyita zone of the South Nations and Nationalities Regional State, Ethiopia. The location and accessibility map of the investigated sites is presented in Fig. 2.

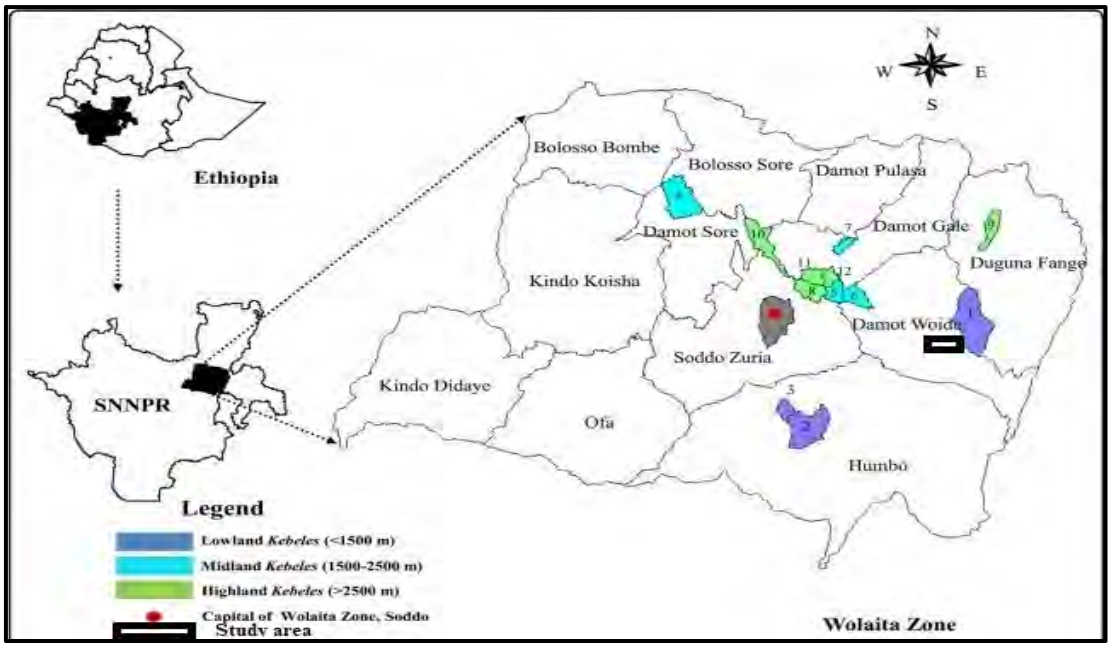

Fig. 2 Location of study area.

2.2 Methodology

2.2.1 An electrical resistivity method

An electrical resistivity is a geophysical technique that amounts to subsurface electrical resistivity configurations using sporadic current with little incidence and a sequence of electrodes inoculated into the pulverized material. An electrode involves current as well as the potential for inoculation (Rehman et al., 2021).

The wholesale resistivity (apparent resistivity) distribution of the subsurface is intended from the capacity based on the electrode structure (Whiteley et al., 2021) and finally upturned to the factual resistivity of the subsurface deposits.

Electrical resistance imaging method was developed within the early decennary. However, they have become increasingly widely used since the Nineteen Seventies, thanks to the provision of computers to method and analyze the information. These techniques area units used extensively to seek appropriate groundwater sources; in engineering, surveys to find subterraneous cavities, faults and fissures; and in anthropology for mapping the regional extent of remnants of the buried foundation of traditional buildings, among several applications (Reyes-Carmona et al., 2021; Morsy and Othman, 2021; Baccani et al., 2021)

The purpose of electrical surveys is to determine the subterraneous electrical resistance distribution by taking measurements on the bottom surface. From these measurements, the electrical resistance will be calculable. The bottom electrical resistance is expounded to various earth science parameters, such as the mineral and fluid content, porosity, nature and degree of water saturation within the rock (Ghanekar, 2021). Vertical electrical sounding (VES) is employed to explore subterraneous lateral and vertical variations in electrical resistance (Ortega et al., 2010).

During this investigation, vertical electrical sounding (VES) information acquisition was utilized victimisation ABEM Terrameter SAS one thousand with Schlumberger conductor configuration at a most current conductor of separation of AB/2 = 150 m.

Apparent electric resistance considers the case wherever this sink at an infinite distance from the supply

(Fig. 3). The potential VC at an enclosed conductor C is that the total of the potential contributions VA and VB from this supply at A and the sink at B may increase by

V_c=V_A-V_B……(1)

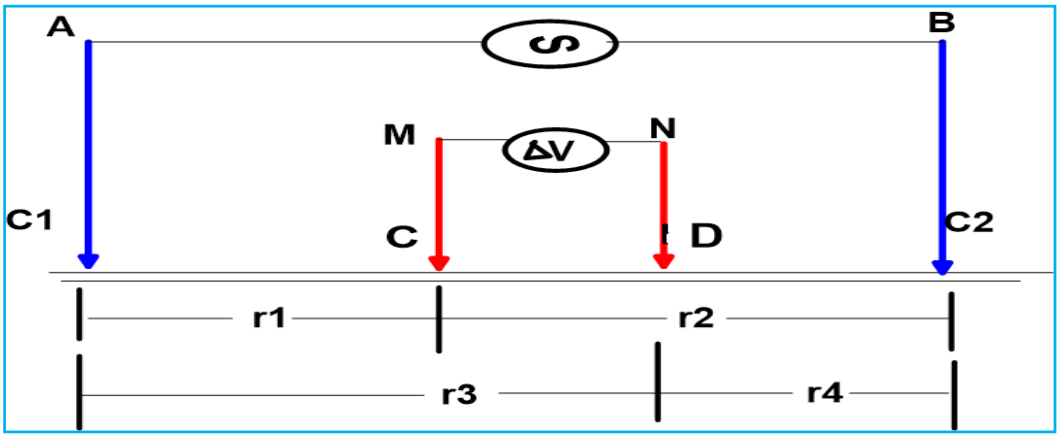

Fig. 3 Apparent electric resistance considers the case wherever the sink at an infinite distance from the supply.

The generalized variety of conductor configuration utilized in the electric resistance survey are two current (C1 and C2) and two potential (M and N) electrodes within the commonplace configuration (Gosar et al., 2021). Now think about the case wherever the higher than conductor layout is placed over solid ground, the voltage measured depends on this applied, the electric resistance of the underwater medium and the geometric issue (k) determined by the array configuration (distance between electrodes). Therefore, mathematically, it is expressed as

$\Delta V = V_C - V_D = \Delta V = V_C - V_D = \frac{I\rho}{2\pi}\left(\frac{1}{r_1} - \frac{1}{r_2} - \frac{1}{r_3} + \frac{1}{r_4}\right)$ ..... (2)

The electric resistance is named apparent electric resistance. The subsequent expression relates these parameters to the apparent resistivity

$\rho_a = k\frac{\Delta V}{I}$ ……..(3)

When mensuration is formed over a solid surface, the apparent electric resistance reaches the electric resistance of the bottom. The apparent electric resistance clearly depends on the pure mathematics of the conductor configuration. The simplest conductor configuration for a field survey depends on the sensitivity of the electric resistance meter, the background signal level, and the relative importance allotted by the geologist to a depth of penetration and lateral resolution. Commonplace conductor configurations used for second UTC surveys area unit Wenner, dipole–dipole, Wenner-Schlumberger, pole-pole, pole-dipole, and equatorial

dipole–dipole (Norooz et al., 2021; Velayudham et al., 2021).

2.2.2 Electrical Resistivity Tomography (2D Imaging)

The DC electric resistance of sounding and identification has with success applied on the side of electric resistance measure in previous however each area unit weak in respect of spatial coverage. Recently, personal computer management and the multi-conductor electric resistance technique have been developed to unravel this weakness in electric resistance measures. The second electrical technique is organized with a totally different array. However, below this investigation, a Wenner array is employed for the field survey. Among the common array sorts, the Wenner array has the strongest signal. The limitation of the electric resistance sounding technique is that it does not take into consideration horizontal modification within the underwater electric resistance. An additional correct model of the underwater electric resistance may be a 2-dimensional second model where the electric resistance changes within the vertical direction, similar to the horizontal direction on the survey line (Fabozzi et al., 2021; Hawke, 2013).

Economical knowledge acquisition is achieved by simultaneously activating many voltages across multiple pairs of electrodes following one injection of electrical current (Arifin et al., 2021). Fig. 2 shows an example of conductor arrangement and mensuration sequence for a second UTC survey.

Once the information acquisition is completed, knowledge analysis is performed victimizing the RES2DINV (Chowdary et al., 2009) code, as well as second pseudo-section plotting and inversion. The RES2DINV rule is represented by Roth et al. (2013) and Abdullah et al. (2022) relies on a smoothness strained statistical method approach.

The DC resistivity of sounding and profiling has successfully applied on the aspect of resistivity 2D electrical method arranged with different array. But under this investigation Wenner array is used to field survey. Among the common arrays types the Wenner array has the strongest signal. Thus the main Ethiopia rift is complex geological settlement due to tectonic and complex volcanic region. The limitation of resistivity sounding method is that does not take into account horizontal change in the subsurface resistivity. A more accurate model of the subsurface resistivity is a two dimensional 2D model where the resistivity changes in the vertical direction as well as horizontal direction along the survey line detected (Loke, 2000).

2.3 Materials

The material that used at field survey in order to primary data collection of ERT and resistivity were described as the following:

- Electrical resistivity meter and its accessary
- Battery
- GPS
- Hammer

2.4 Data acquisition techniques

In order to acquire data for this study, the electrical resistivity (VES and ERT) methods were used to measure the apparent resistivity data in one and two dimension respectively (Figs 4 and 5).

2.4.1 Vertical electrical sounding data acquisition

The electrical resistivity measurement is procedure of sending signal by current electrodes to the ground and measuring potential at other electrodes in the vicinity of current flow. Vertical electrical sounding (VES) used to detect the variation of resistivity values of the geological units with depth. During the field survey for VES data acquisition Schlumberger array was used and arranged with two current electrodes and two potentials electrodes. This array was adjusted for measurement, laid the resistivity tiara meter at center and expands current electrodes in both directions to detect resistivity of subsurface with depth.

Two profiles of VES data points were taken from field survey by resistivity tiara meter. The first profile

line has two VES (DamVES1, Dam VES2) and its data were acquired Northwestern to Southeastern direction. The second profile line consists of two VES (VES2, VES7) data points that were taken along southwestern to northeastern trends. The horizontal distance of current electrode ($\frac{AB}{2}$) for each VES profile was 150 m and the separation distance between each VES data point of the first profile line adjusted at intervalof140m.The Schlumberger electrode configuration was used for VES measurements in all explored sites with the maximum current probe parting array used 150 m (half - the maximum current electrode separation) and was conducted along two lines which are about 140 m apart. The VES were carried out with maximum current probe laying (AB/2) of 150 meters by smearing electrical current into the earth by means of two current electrodes, and the resulting potential difference was measured by the pair of potential electrodes located in the center. The current electrode arrangement designated for these surveys was AB/2 (1.5, 2.1, 3, 4.2, 6, 9, 13.5, 20, 30, 45, 66, 100 and 150) meters and the spacing of the potential electrodes was MN/2 (0.5, 6, and 45) meters. The repeated measurements are taken at 20, 30 150 and 220 m in order to remove ambiguity. Each value of the resistivity and the adjusted interval values of AB/2 and MN then recorded on the paper manually and finally transferred it into computer. Then, Ipi2win, and surfer software were used to interpret the resistivity values qualitatively and quantitatively.

2.4.2 Electrical resistivity tomography data acquisition

The electrical resistivity tomography (ERT) data was acquired by using SYSCAL PRO instrument, which is the same instrument employed for VES data acquisition. It involves multi core cables which contain as many individual wires as number of electrodes. For this survey the instrument utilized with 72 electrodes through inter connect able of four reel cables accommodating 18 electrodes for each cable, 72 short connector wires and two reversible connector boxes. The cables used in particular adjusted at connection point by interval (space) of 10 m. The reel cable are connected to each other with connector boxes and each cable outlet is connected to the electrode by the connector wires of twelve voltage of external battery was used for power supply to the instrument. The instrument is normally put at the center of the four reel cables and expands these four reel cables in both sides of the instrument. Two reel cables along one side and the rest two cables are along the other side.

The instrument was recorded data automatically with a format of uploaded into the unit and the system takes the measurement was at adjusted time of 45 minute for each profile. After finish the recording of the data was saved in internal memory at specific location and then transferred to the computer by using of USB cable.

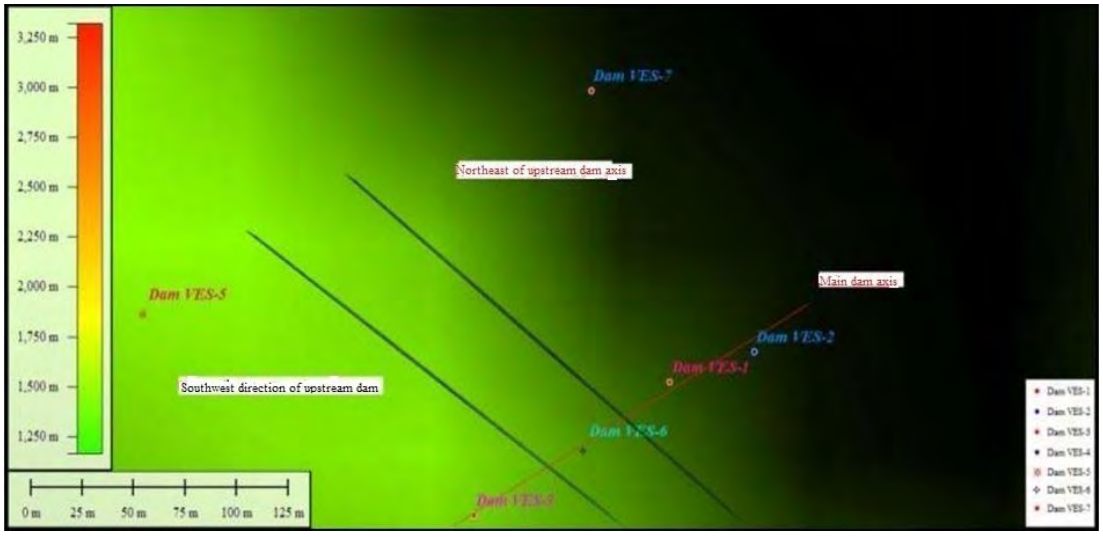

Fig. 4 Digital map of the AnkaShasha investigated sites on the Chirostream.

Fig. 5 Photographic view of vertical electrical sounding (a) and electrical imaging tomography (b).

3 Results and Discussion

3.1 Vertical Electrical Sounding (VES)

Analysis and interpretation of field data, as well as result writings, were carried out using different software. Likewise, all VES data were interpreted in terms of layer parameters (depth, thickness and resistivity) with the aid of IPI2 win and Ix1D Version 2.8 software, which is specially designed for vertical electrical sounding (VES) and/or induced polarization data curves 1D interpreting along with a single profile. It is presumed that the user is an experienced interpreter willing to solve all geological problems and/or challenges as well as to fit the sounding curves.

Topographic data along the traverses were extracted from the Shuttle Radar Topographic Mission (SRTM) data set. The maps and Geoelectric Resistivity Sections were generated by means of a digital elevation model (DEM) and global mapper. Data plotting, analysis and report writing were performed using Microsoft Office (Word, Excel Surfer).

The vertical electrical multilayer sounding field curves obtained once curve matching and laptop iteration showed numerous varieties of curves that were determined by the connection existing formation layer thickness station between the layer electrical phenomenon values ρ1, ρ2, ρ3 and ρ4. It was discovered that the curves are principally HA-type curves with the exception of seven of a kind of KH. A summary of the formation layer thickness, classification of the electrical phenomenon sounding and samples of the curves are given in the Table 1.

Table 1 Location of DAM Tra1 along Dam VES-1 and Dam VES-2 on the traverse route.

S. No.	VES type	Easting	Northing	Altitude (AMSL)
1	Dam VES-1	390002	762357	1455
2	Dam VES-2	390043	762370	1457

The Tral with NE-SW headings shows two major resistivity groups. The first group characterized by 5-870 Ohm-m resistivity is clearly delineated under VES points Dam VES-1, and Dam VES-2 interpreted as compact dry

clay topsoil, moderately to slightly weathered tuff and fractured Ignimbrite where the registered average depth extent is 5-15 m. The second group with a range of resistivity value of 800-1150 Ohm-m presumably related to and interpreted as slightly weathered\fractured Ignimbrite (bedrock) distinctive to the area of Dam VES-2 at 29 meters. Interpreted and summarized data of VES point Dam VES-1 and VES-2 are listed in Table 2 and 3.

Table 2 Interpreted and summarized data of VES point Dam VES-1.

Layer	Resistivity (Ωm)	Depth (m)	Expected lithology
1	33-711	0-15	Topsoil, weathered ash, and an outcrop welded tuff
2	1158	15-29	Slightly weathered and fractured Ignimbrite.
3	5	>29	Weathered ash/tuff (saturated).

Table 3 Interpreted and summarized data of VES point Dam VES-2.

Layer	Resistivity (Ωm)	Depth (m)	Expected lithology
1	30-871	0-5	Topsoil weathered ash and outcrops dry welded tuff
2	591	5-13	Slightly weathered and fractured Ignimbrite.
3	13	>29	Weathered ash/tuff (saturated)

The topography path and resistivity profile along Dam VES-2 and Dam VES-7 and the resistivity graph and geo-electric parameter (model) of Dam VES-2 are depicted in Figs 6 and 7.

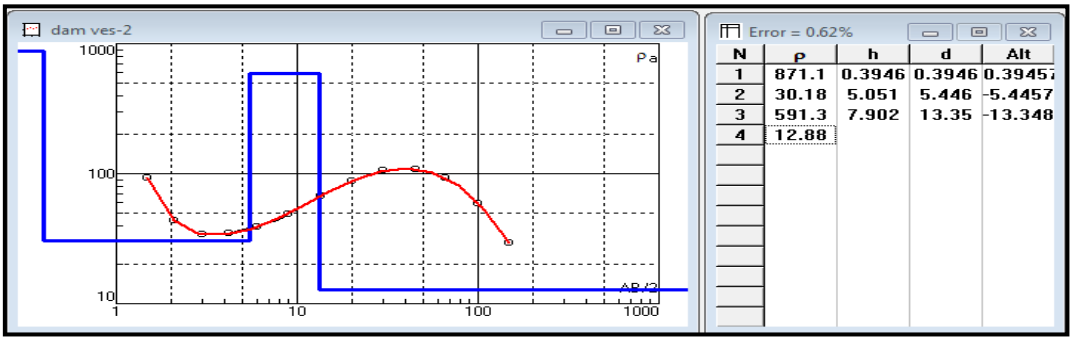

Fig. 6 Resistivity graph and geo-electric parameter (model) of Dam VES-2.

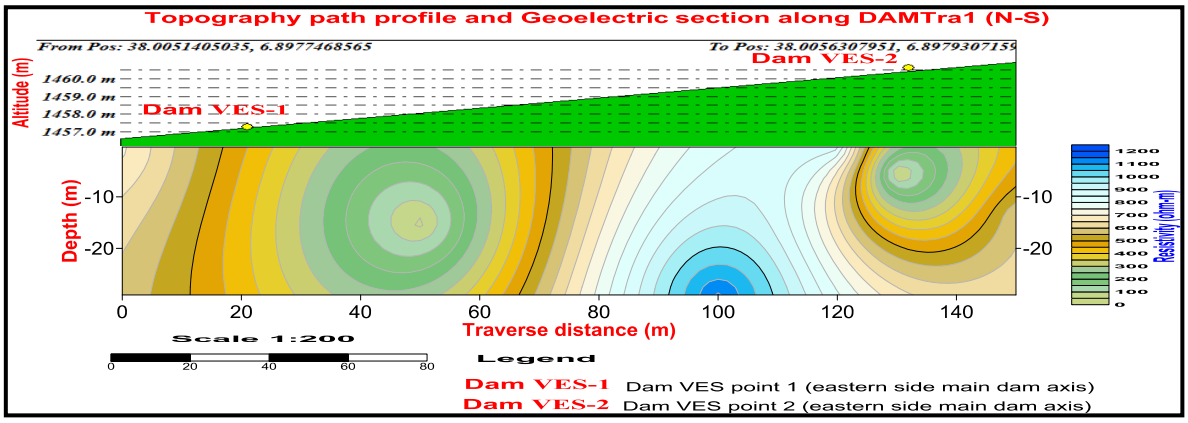

Fig. 7 Topography path profile and geo-electric section along Dam VES-1 and Dam VES-2.

The traverse obtained along Dam VES-2 (considered again) with Dam VES-7 (upstream) was to analyze and correlate the result obtained from the above DAM Tra1. Location of DAM Tra2 along Dam VES-2 and Dam VES-7 on the traverse route,and interpratations are listed in Table 4 and 5, respectvely.

Table 4 Location of DAM Tra2 along Dam VES-2 and Dam VES-7 on the traverse route.

S. No.	VES type	Easting	Northing	Altitude (AMSL)
1	Dam VES-2	390043	762370	1457
2	Dam VES-7	389964	762484	1468

Table 5 Interpreted and summarized data of the VES-7 point eastern flank of the upstream axis.

Layer	Resistivity (Ωm)	Depth (m)	Expected lithology
1	29	0-3	Dry topsoil, weathered ash and an outcrop welded tuff
2	679	3-6	Slightly weathered and fractured Ignimbrite.
3	52	6-32	Weathered tuff, ash and pumice
4	27	>32	weathered ash and tuff (saturated)

The geo-electric resistivity section obtained along Traverse Route DAM Tra2 (Fig. 8) from the main dam axis to upstream of the reservoir area with NE-SW headings shows three major resistivity groups. The first group characterized by 5-350 Ohm-m resistivity is clearly delineated under VES points Dam VES-1 and Dam VES-2 interpreted as compact dry clay topsoil, highly to moderately weathered tuff and fractured Ignimbrite where the registered average depth extent is 5-15 m (Bergman et al., 2013). The second group with an average resistivity value of 450 Ohm-m resistivity response is interpreted as slightly weathered\fractured Ignimbrite\ rhyolite limited to the area of MS VES-1 near the surface. The third group, with an average resistivity value of 650-850 ohm-m resistivity, presumably basement (bedrock) lithological related to and interpreted as slightly weathered/fractured.

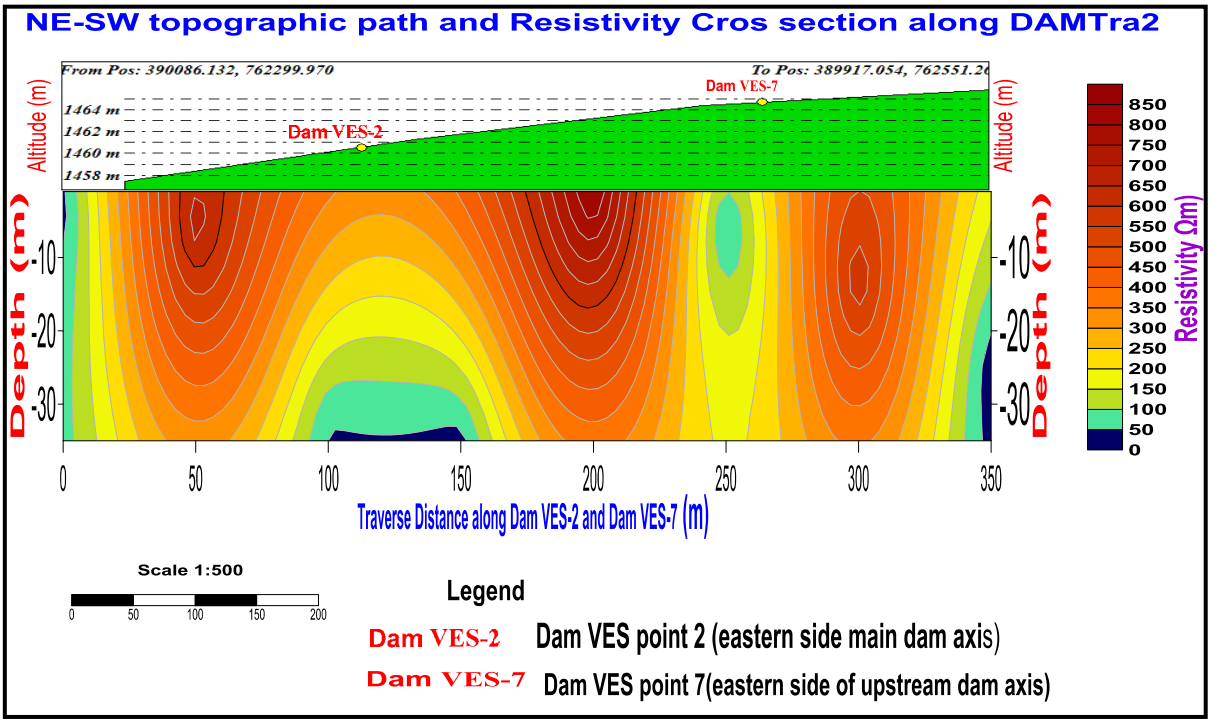

Fig. 8 Topography path and resistivity profile along Dam VES-2 and Dam VES-7.

3.2 Two-dimensional (2D) electrical resistance imaging surveys

Two dimensional (2D) electrical imaging surveys area unit currently wide accustomed map of area unit as moderately advanced earth science wherever 1D resistivity sounding surveys are inadequate. The RES2DINV program uses the smoothness-constrained least sq. technique inversion technique to provide the second belowground model from apparent electrical resistance knowledge. Figs 9, 10 and 11 show an electrical imaging survey in a locality with fairly advanced belowground earth science and important surface topography of the AnkaShasha dam site. Resistivity imagings ASDAMI profile-1 across the EW downstream of the dam axis area survey are listed in Table 6.

Table 6 Resistivity imaging ASDAMI profile-1 across the EW downstream of the dam axis area.

S. No	Resistivity Imaging type	Easting	Northing	Altitude (AMSL)
1	ASDAMI profile-1	390002	762215	1431

3.2.1 Geo-electric resistivity imaging section ASDAMI profile-1

The first group characterized by 5-61 Ohm-m resistivity is clearly delineated under this geo-electric imaging section interpreted as sand clay where the average depth extent varies from 1.25-24 erratically as shown in figure 9 topsoil, highly to moderately weathered tuff and fractured Ignimbrite where the registered average depth extent is 1-15 m. The second cluster with a median electrical resistance price of 140-319 Ohm-m electrical resistance response is understood as from extremely to moderately weathered\fractured Ignimbrite/basalt to a median depth of 8-24 at the sting the natural stream depression and pinch out at the stream natural depression floor (Hokkanen et al., 2010). The third cluster, with a median electrical resistance price larger than 729-1665 Ohm-m electrical

resistance, presumptively slightly broken and weather-beaten basement (bedrock) to a depth of 22-24 meters. Survey values of resistivity imaging ASDAMI profile-2 along the floor upstream of the dam axis are listed in Table 7.

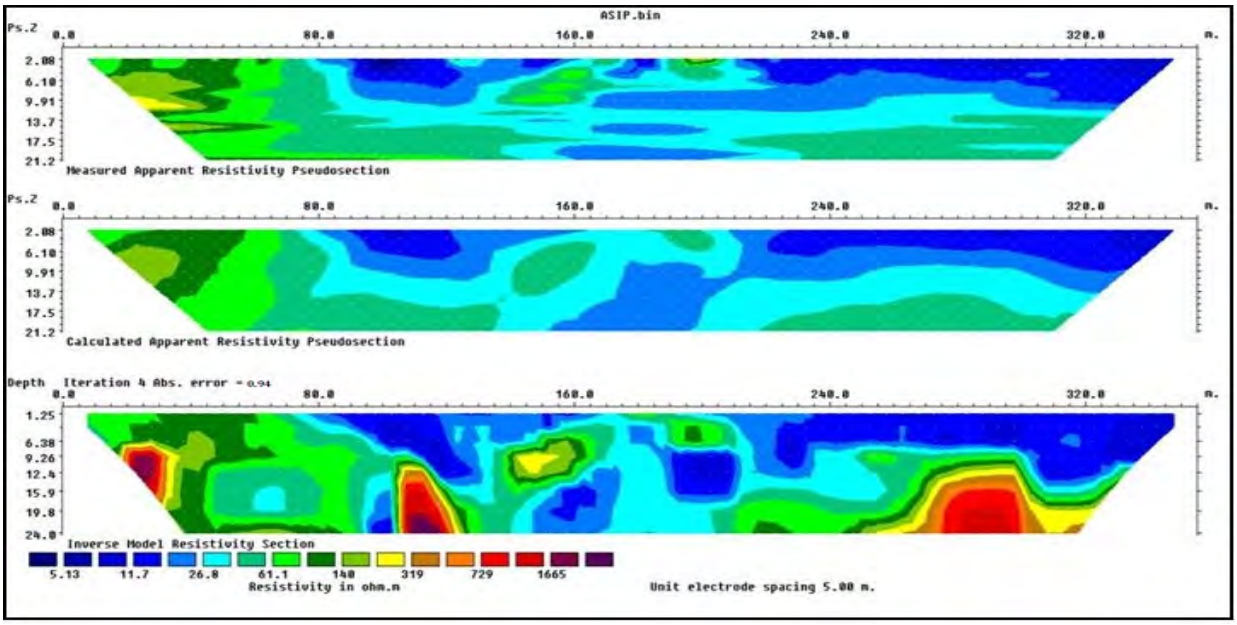

Fig. 9 Typical display output and intended apparent resistivity virtual sections and the overturn model segment.

Table 7 Resistivity imaging ASDAMI profile-2 along the floor upstream of the dam axis.

S.No.	Resistivity Imaging type	Easting	Northing	Altitude (AMSL)
1	ASDAMI profile-2	389925	762364	1448

3.2.2 Geo-electric resistivity imaging section ASDAMI profile-2

The first group characterized by 3-71 Ohm-m resistivity is clearly delineated under this geoelectric section interpreted as compact dry clay topsoil, highly to moderately weathered tuff and fractured Ignimbrite where the registered average depth extent is 1-12 m. The second group with an average resistivity value of 1349-4889 Ohm-m resistivity response is interpreted as from slightly weathered\fractured Ignimbrite to an average depth of 19 (Aktaş et al., 2021). The third group, with an average resistivity value of 17148 ohm-m resistivity, presumably fresh basement (bedrock) lithologically related to and interpreted as fresh Ignimbrite to a depth of 24 metres. Location of MKD Tra2 along MK dam VES-5 and MK dam VES-6 on the traverse route are listed in Table 9.

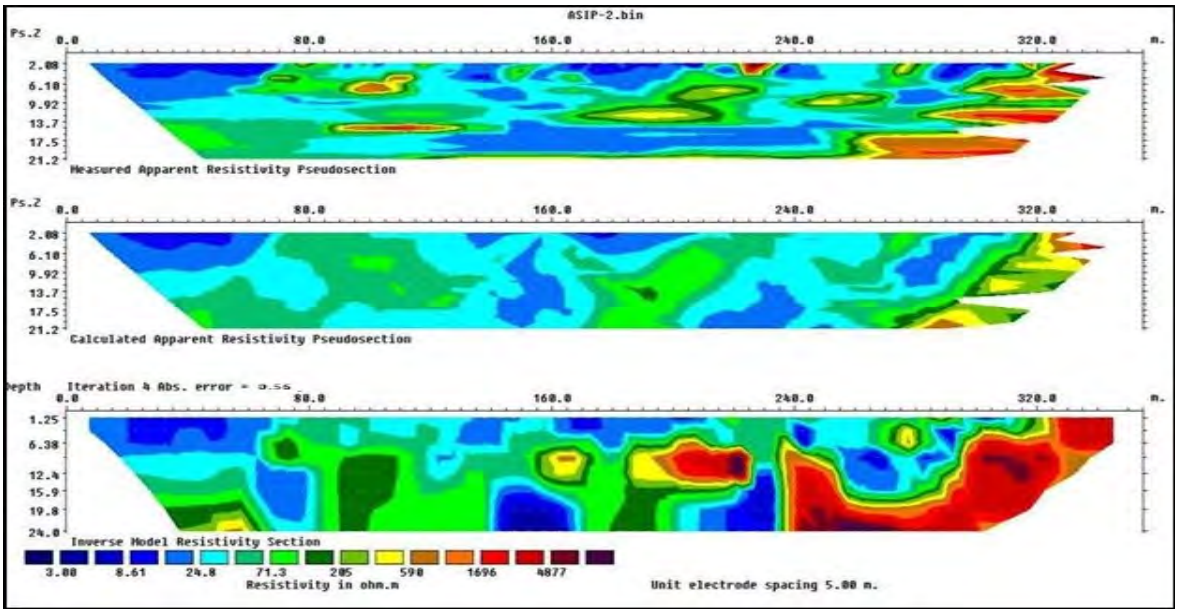

Fig. 10 Typical display output showing the measured and calculated seeming resistivity pseudo-segments and the overturn model segment.

Table 7 Location of MKD Tra2 along MK Dam VES-5 and MK Dam VES-6 on the traverse route.

S.No.	Resistivity Imaging type	Easting	Northing	Altitude (AMSL)
1	ASDAMI profile-3	389904	762396	1436

3.2.3 Geo-electric resistivity imaging section ASDAMI profile-3

The first group characterized by 3-14 Ohm-m resistivity is clearly delineated under this geo-electric imaging section interpreted as wet sand and clay where the average depth extent varies from 1.25-24 erratically as shown on figure topsoil, highly to moderately weathered tuff and fractured Ignimbrite where the registered average depth extent is 1-15 m. The 2nd collection with an average resistivity value of 148-550 Ohm-m resistivity response is interpreted as from moderately to slightly weathered\fractured Ignimbrite/basalt to an average depth of 8-24 at the edge of the stream valley and pinch out at the stream valley floor (Ulysse et al., 2021).

The third group, with an average resistivity value greater than 1665 ohm-m resistivity, presumably fresh basement (bedrock) lithologically related to and interpreted as fresh Ignimbrite to a depth of 24 metres (Zhou et al., 2021). Topographic path profile of the main dam axis with VES points are depicted in Fig. 12.

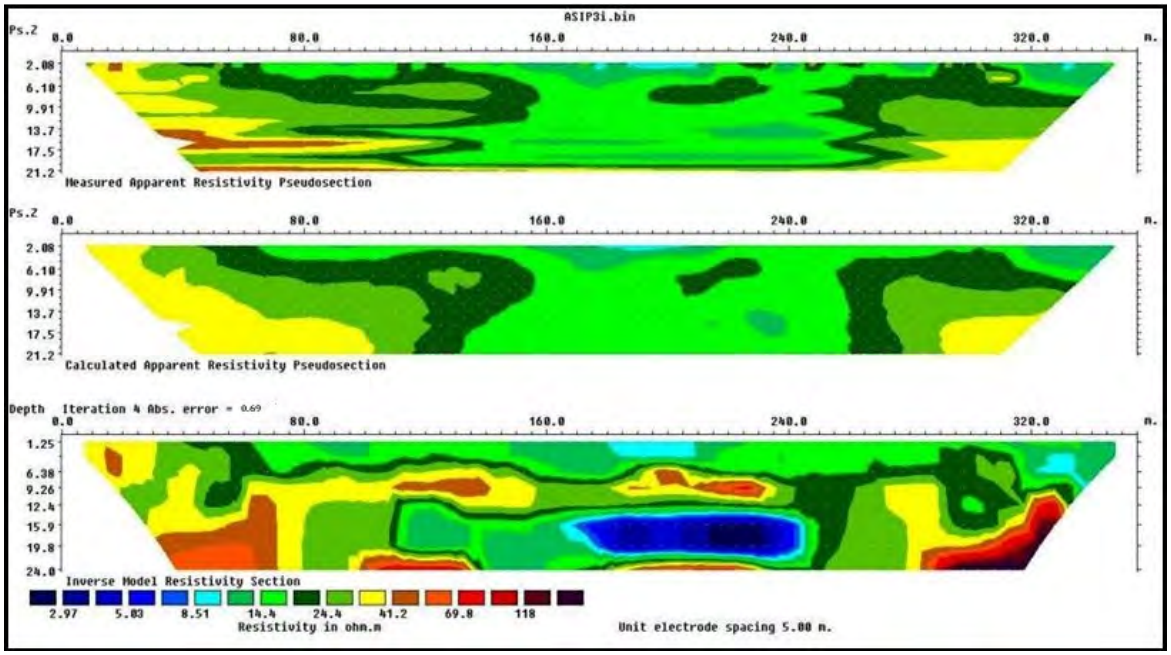

Fig. 11 Typical display output and calculated seeming resistivity pseudo-segments and the inversion model segment.

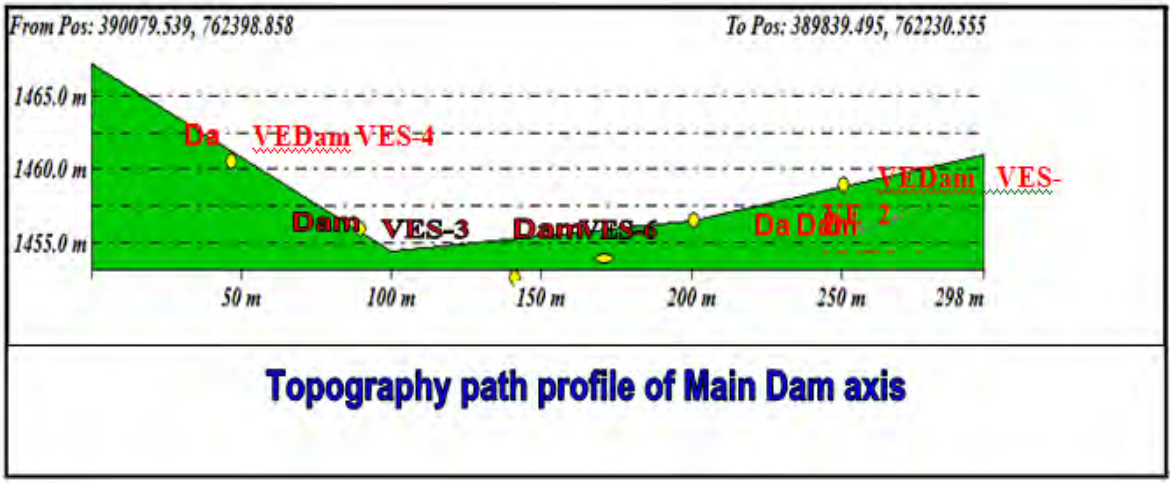

Fig. 12 Topographic path profile of the main dam axis with VES points.

4 Conclusion and Recommendations

4.1 Conclusion

Geophysical surveys, Vertical Electrical Sounding (VES) and two-dimensional (2D) electrical impedance imaging surveys were carried out to investigate the dam. The data were processed on the IPI2win impedance software system, conferred within the sort of sections distance depth, within the sort of inversion model in terms of electrical impedance profile. The inversion method consists of a series of 4-5 layers. The layout of the layers is joined to the distribution of knowledge points on a geo electric section, i.e., the section generated in-depth with taken impedance field information. The summaries of the interpretation results of the sounding curves obtained from the planned dam axis in terms of the impedance profile/geo electric/geologic layering are conferred within the top figures.

VES was conducted at the NE flank of the dam on the most and upstream (reservoir) space. The skinny layer soil that consists of sandy clay associated with Nursing clayey sand and outcrops of welded volcanic rock and Ignimbrite is clearly manifested close to the surface and is outlined by layer impedance values varying from five to 800 Ω-m with depth ranges from 5 to 15 meters. Moreover, the geo electric characteristics of the bedrock on the jap flank gift slightly weather-beaten and facture basement characteristics obtained on DAMtra1 and DAMTRA2 consist of Ignimbrite with impedance worth varying from 850 to 1150 Ω-m whereas the thickness varies from 13 to 29 m. While investigating traverse, DAMTRA1 was selected to hide the waste weir of the dam. The waste weir is characterized by the broken sign of comparatively high impedance, as shown in figure a pair around Dam VES-1 and Dam VES-2 space.

Meanwhile, VES was conducted at the point flank of the dam on the most and upstream (reservoir) space, and the skinny layer soil, which consists of sandy clay and clayey sand and extremely to moderately weather-beaten welded volcanic rock and broken Ignimbrite, is clearly manifested at depths comparatively deeper (up to 25 m) than the NE flank of the stream and is outlined by layer impedance values varying from four to three hundred. The low impedance zone LRZ-1 within the dam of AnkaShasha is the most visible zone in the electrical impedance profile model. The intensity and size of the zone are higher on the western flank of the main dam and upstream than on the jap flank of the main dam axis and upstream (reservoir area). The stream channel with a low impedance zone (LRZ) is the most visible channel in the electrical impedance profile model (Fig. 11), wherever the intensity and size of the zone are on top of the upstream space, presents no detectable broken basement (bedrock) characteristics because of the bedrock on the jap and western flank of the stream.

The bedrock is nearer to the surface on the painted fracture boundaries on the geo electric section of NE flanks of the axis. The overburdened materials consist of flow paths that widen northeastwards parallel to clay, sandy clay and clayey sand. Therefore, the jap flank of the stream usually dries, as shown within the comparatively high impedance website (upstream axis). Subsequent to the positioning visit, the determined gullies are assumed to be the flow because of the underlying broken rock sub drain system. The fractures are clearly shown at a lower place in the upstream and main dam planned reservoir space. However, some sort of correction within the style method is needed to reduce the threat exhibited by the existence of fractures that are potential underground flow channels, as shown on the impedance profile. Therefore, it is possible to affirm that the study presents approximately satisfactory results, even though not the foremost excellent, and conclude that geology represents a cheap variety for the review of earth dams. However, the utilization of alternative geology methods and core drilling will aid within the identification of potential structures and add larger quality to the results.

4.2 Recommendation

Seismic refraction work: should be forwarded since the area is seismically active to map the structures and determine parameters such as densities of each layer, depth to contacts and others. Implements of the above recommended geophysical methods should be supplemented by other studies from a related field. Integrating the geophysical results into hydrogeological and geo-structural methods is mandatory for the safety of the dam.

References

Abdullah F. 2022. Utilizing NWCR optimized arrays for 2D ERT survey to identify subsurface structures at Penang Island, Malaysia. Journal of Applied Geophysics, 196: 104518

Abotalib A. 2021. Groundwater mounding: A diagnostic feature for mapping aquifer connectivity in hyperarid deserts. Science of The Total Environment, 801: 149760

Aktaş G, Hisarli Z, Demirel A. 2021. High-resolution total field magnetic anomaly maps of Lake İznik (NW Turkey): assessment of faults which play important roles in tectonics of the lake. Marine Geophysical Research, 423(42): 1-17

Arifin M. 2021. Environmental hazard assessment of industrial and municipal waste materials with the applications of RES2-D method and 3-D Oasis Montaj modeling: A case study at Kepong, Kuala Lumpur, Peninsula Malaysia. Journal of Hazardous Materials, 406: 124282

Baccani G. 2021. The reliability of muography applied in the detection of the animal burrows within River Levees validated by means of geophysical techniques. Journal of Applied Geophysics, 191: 104376

Bergmann P. 2013. Combination of seismic reflection and constrained resistivity inversion with an application to 4D imaging of the CO_2 storage site, Ketzin, Germany. Geophysics, 72(2): B37-B50

Chowdhury A, Jha MK, Chowdary VM. 2009. Delineation of groundwater recharge zones and identification of artificial recharge sites in West Medinipur district, West Bengal, using RS, GIS and MCDM techniques. Environ. Earth Science, 59: 1209-1222

Cox M, James A, Hawke A, Raiber M. 2013. Groundwater Visualization System (GVS): A software framework for integrated display and interrogation of conceptual hydrogeological models, data and time-series animation. Journal of Hydrology, 491: 56-72

Fabozzi S. 2021. Stochastic approach to study the site response in presence of shear wave velocity inversion: Application to seismic microzonation studies in Italy. Engineering Geology, 280: 105914

Fisseha S, Mewa G, Haile T. 2021. Refraction seismic complementing electrical method in subsurface characterization for tunneling in soft pyroclastic, a case study. Heliyon, 7: e07680

Gamidi S, Ghanekar R. 2021. Integrated Geophysical and Geotechnical Study of a Southern Oil and Gas Field in Western Offshore, India. Health and Environment Research Online, 575-588

Ge L. 2021. Current Trends and Perspectives of Detection and Location for Buried Non-Metallic Pipelines. Chinese Journal of Mechanical Engineering, 341(34): 1-29

Mollehuara-Canales R, Kozlovskaya E, Lunkka JP, Moisio K, Pedretti D. 2021. Noninvasive geophysical imaging and facies analysis in mining tailings. Journal of Applied Geophysics, 192: 104402

Morsy E, Othman A. 2021. Delineation of shallow groundwater potential zones using integrated hydrogeophysical and topographic analyses, western Saudi Arabia. Journal of King Saud University, 33: 101559

Norooz R, Olsson P, Dahlin T, Günther T, Bernstone C. 2021. Geoelectricalprestudy of Älvkarleby test embankment dam: 3D forward modeling and effects of structural constraints on the 3D inversion model of zoned embankment dams. Journal of Applied Geophysics, 191: 104355

Ortega A, Benito-Calvo A, Porres J, Pérez-González A, Martín Merino M. 2010. Applying electrical resistivity tomography to the identification of endokarstic geometries in the Pleistocene Sites of the Sierra de Atapuerca (Burgos, Spain). Archaeological Prospection, 17: 233-245

Pezdir V, Čeru T, Horn B, Gosar M. 2021. Investigating peatland stratigraphy and development of the Šijec bog (Slovenia) using near-surface geophysical methods. CATENA, 206: 105-484

Pilecki Z. 2021. Identification of buried historical mineshaft using ground-penetrating radar. Engineering Geology, 294: 106400

Placencia-Gómez E, Parviainen A, Hokkanen T, Loukola-Ruskeeniemi K. 2010. Integrated geophysical and geochemical study on AMD generation at the Haveri Au–Cu mine tailings, SW Finland. Environ. Earth Science, 617(61): 1435-1447

Rehman. 2021. Shallow geophysical and hydrological investigations to identify groundwater contamination in Wadi Bani Malik dam area Jeddah, Saudi Arabia. Open Geosciences, 13: 272-279

Reyes-Carmona. 2021. Rapid characterization of the extremely large landslide threatening the Rules Reservoir (Southern Spain). Landslides, 18: 3781-3798

Roth G. 2013. Water-use efficiency and productivity trends in Australian irrigated cotton: a review. Crop and Pasture Science, 64: 1033-1048

Ulysse S. 2021.Site effect potential in Fond Parisien, in the East of Port-au-Prince, Haiti. Natural Geoscience, 11: 175

Velayudham J. 2021. Comprehensive study on evaluation of Kaliasaur Landslide attributes in Garhwal Himalaya by the execution of geospatial, geotechnical and geophysical methods. Quaternary Science Advances, 3: 100025

Whiteley JS, et al. 2021. Rapid characterization of landslide heterogeneity using unsupervised classification of electrical resistivity and seismic refraction surveys. Engineering Geology, 290: 106189

Zhang L, Xu L, Xiao Y, Zhang NB. 2021. Application of comprehensive geophysical prospecting method in water accumulation exploration of multilayer goaf in integrated mine. Advances in Civil Engineering, 2019: 2368402

Zhang W, et al. 2021. Optimization design and assessment of the effect of seepage control at reservoir sites under karst conditions: a case study in Anhui Province, China. Hydrogeology Journal, 29: 1831-1855

Zhou X. 2021. Crustal architecture and structural evolution of a Neoarchean sedimentary basin: geological and geophysical evidence from Metal Earth Chicobi transect in the Abitibi Subprovince, Superior Province, Quebec, Canada. Precambrian Research, 365: 106391